Kinetics and Catalysis, Vol. 46, No. 2, 2005, pp. 177–188. Translated from Kinetika i Kataliz, Vol. 46, No. 2, 2005, pp. 191–202.

Molecular Mechanism of Direct Alkene Oxidation with Nitrous Oxide: DFT Analysis

V. I. Avdeev, S. F. Ruzankin, and G. M. Zhidomirov

Boreskov Institute of Catalysis, Siberian Division, Russian Academy of Sciences, Novosibirsk, 630090 Russia

Received February 26, 2004

Abstract—Reaction paths are calculated by the DFT method in the B2LYP/6-31G* approximation for direct oxidation of cyclohexene and butene with nitrous oxide into carbonyl compounds. Two possible reaction channels differing in their intermediate are analyzed. Two-step mechanisms are predicted for these reactions. Both steps are activated reactions. The first step of the first channel is the conversion of the initial reactants into the five-membered heterocycle 1,2,3-oxadiazole, –C–N=N–O–C–, via a transition state. The first step of the second channel leads from the reactants via a transition state to a three-membered heterocycle (epoxide), –C–O–C–. The second step is the decomposition of these intermediates through hydrogen transfer within the hydrocarbon backbone and the formation of the final products. The rate-limiting step in the oxidation of cyclohexene and butene is determined by the electronic structure of the –C–N=N–O–C– heterocycle and is independent of the structure of the other hydrocarbon moieties. The activation energies calculated for separate steps suggest that the first reaction channel, leading to carbonyl compound, is more favorable from the standpoint of energetics. Two reaction pathways are possible for butene-1 oxidation, one leading to a ketone and the other to an aldehyde. The ketone is predicted to dominate in the product.

Nitrous oxide is a promising oxidant, and its use in the selective oxidation of hydrocarbons has attracted researchers' attention [1]. In recent years, interest in this process has grown because of the environmental problem of utilizing N_2O emissions [2]. Although the N_2O molecule is thermodynamically unstable and decomposes readily into dinitrogen and oxygen, the high activation barrier makes it kinetically rather stable up to 1000°C. The activation barrier for gas-phase N_2O decomposition,

$$N_2O \longrightarrow N_2 + O(^3P) + \Delta_r H_0^0 \qquad \text{(I)}$$

was experimentally estimated at 50–60 kcal/mol [3]. Although spin-forbidden, reaction (1), characterized by an enthalpy change of $\Delta_r H_0^0$ = 39 kcal/mol, is thermodynamically much more favorable than the formation of singlet oxygen $O(^1D)$ ($\Delta_r H_0^0$ = 84 kcal/mol). Due to the metastability of its molecule, N_2O is a preferable oxidant for hydrocarbons from the standpoint of energetics. Indeed, for the formation of CH_3OH from CH_4 and of PhOH from PhH, $\Delta_r H_{298}^0$ = –50 and –62 kcal/mol, respectively [2]. However, implementation of oxidation processes involving nitrous oxide requires N_2O to be activated. Aside from spectral excitation, the most natural way of doing this is by using a catalyst. The N_2O molecule can be markedly destabilized by adsorption on an active site (AS). In the limiting case, this interaction can initiate a direct dissociation of the molecule to N_2 and an oxygen atom bound to the AS:

$$N_2O\text{–(AS)} \longrightarrow N_2(\text{gas}) + \text{O–(AS)}. \qquad \text{(II)}$$

This reaction can probably be carried out with various heterogeneous catalysts at moderately elevated temperatures. For example, with a catalytic system based on the high-silica zeolite FeZSM-5, reaction (II) sets in at $T \geq 150$°C [4].

A number of studies have been devoted to theoretical analysis of reaction (II) for various catalysts and AS models. For example, a wide variety of transition metal atoms ranging from Sr to Cu were considered as AS's [5]. The monoatomic iron ions Fe^{1+} [6], Fe^{2+} [7], and Fe^{3+} [8] at the cationic sites of high-silica zeolites have also been discussed. Oxide–hydroxide models were analyzed for Fe^{3+}, Co^{3+}, Rh^{3+} [9], and Al^{3+} [10]. The purpose of this modeling could have been description of the AS's in the respective metal oxides and in extralattice oxide–hydroxide species in the zeolite matrix. The latter case was considered in terms of a dinuclear Fe^{3+} cluster model [11, 12]. Calculations were carried out for Fe^{2+} and Fe^{3+} in dinuclear bridged oxide structures stabilized by cationic sites in FeZSM-5 [13]. The energy of the resulting O–AS bond, $E_{O–AS}$, is of great significance in the analysis of both catalyst-induced N_2O decomposition and the activity of the O–AS structure in substrate oxidation. A rather large $E_{O–AS}$ value is necessary for reaction (II) to take place at moderate

0023-1584/05/4602-0177 © 2005 MAIK "Nauka/Interperiodica"

temperatures. Conversely, the oxidizing activity of an O–AS structure increases with decreasing E_{O-AS}. Another requirement that must be met by the optimum value of E_{O-AS} is minimization of the complete decomposition reaction $2N_2O \longrightarrow 2N_2 + O_2$ under selective substrate oxidation conditions. These requirements define a rather narrow range in which the catalytic activation of N_2O is possible. For the FeZSM-5 catalyst, ~60 kcal/mol [4]. This value apparently falls within the optimal energy range. This catalyst, developed by Panov and his colleagues [1], was used by Solutia Co. (the United States) in direct benzene oxidation with nitrous oxide into phenol.

An essential problem in the oxidation of various hydrocarbons with nitrous oxide on this catalyst is desorption of the reaction products. Analysis of the mechanism of benzene oxidation into phenol at the model site Fe^{2+} in FeZSM-5 predicts a rather high energy of $E \sim 24$ kcal/mol [7] for the bond between the resulting phenol and the AS. This value is in strong agreement with experimental data. Therefore, the reaction has to be conducted at an elevated temperature. An attempt to carry out this reaction in the liquid phase was successful only in part. However, direct noncatalytic alkene oxidation with nitrous oxide into carbonyl compounds was found to be possible [14–16].

As mentioned above, the main factor restricting N_2O application as an alternative hydrocarbon oxidant in the absence of a catalyst is the high activation energy of N_2O decomposition. Because of this, the reaction has to be conducted at a high temperature and, as a consequence, oxidation is low-selective. Apparently, studies by Bridson-Jones and Buckley [17–19] were the first purposeful attempt to reduce the reaction temperature. Those researchers demonstrated that, at $T \sim 300$°C and pressures up to 500 atm, N_2O oxidizes the C=C bond in hydrocarbons to yield carbonyl compounds. However, even in the case of cyclohexene, which is the most selectively oxidizable compound, cyclohexanone selectivity did not exceed 60%. A wide variety of other organic compounds (paraffins, cycloparaffins, arenes, amines, and ethers) turned out to be inoxidizable under the above conditions. It was probably because of the insufficient oxidation selectivity that the results of those studies did not find any application. Panov *et al.* [14–16] have recently demonstrated that selective alkene oxidation with nitrous oxide into carbonyl compounds can take place in the liquid phase without catalyst mediation at 150–250°C.

Unlike Bridson-Jones *et al.* [17, 18], Panov and his colleagues [14–16] achieved a high selectivity (98–100% for some alkenes) and a comparatively high reactant conversion in this reaction. This promising result was obtained by conducting the reaction in the liquid phase to rule out uncontrollable gas-phase reactions, which could have caused side reactions and, as a consequence, a decrease in selectivity. This finding provides grounds for hoping that N_2O will soon find application as an active donor of atomic oxygen in important oxidations.

Five-membered heterocycles are widely synthesized by 1,3-dipolar cycloaddition [20]. A number of theoretical studies are devoted to this method of reacting N_2O with alkenes. For example, reaction path calculations for cycloaddition reactions between 16-electron 1,3-dipoles (N_2O, N_2NH, N_2CH_2, etc.) and ethylene are presented in a recent paper [21] (which contains a comprehensive survey of relevant theoretical and experimental studies). It is demonstrated in that report that all of these reactions pass through a transition state with an activation energy of 13–20 kcal/mol. There have been no reports on the subsequent transformations of the five-membered heterocycles into products of selective hydrocarbon oxidation. Here, we attempt a theoretical analysis of this issue. Based on reaction path calculations for direct alkene oxidation with nitrous oxide, we interpret some previous experimental findings [14–16] and suggest a molecular mechanism for this type of reaction. We consider cyclohexene as a cyclic alkene and butene-1 and butene-2 as aliphatic alkenes.

COMPUTATIONAL METHODS

Determination of the reaction path includes optimization of the structures of the initial reactants (R), reaction products (P), possible intermediates (Int), and transition states (TS) as a first step. The second step is calculation of normal mode frequencies for all of the optimized structures, including the transition states. Next, imaginary frequencies at saddle points are analyzed and the energy profile as a function of the reaction coordinate is calculated using the IRC method [22]. All calculations were made in the DFT framework [23]. This method found wide application in the calculation of the electronic structure of molecules after efficient algorithms had been developed for calculating the exchange correlation energy E_{xc} in the Kohn–Sham equation [24]. The essence of these approximations is that gradient corrections to the exchange and correlation energies are made. We used the so-called hybrid B3LYP method suggested by Becke [25, 26], in which the standard Hartree–Fock exchange energy is about 20% and the gradient corrections to the exchange energy are separated as a B88 functional. The Lee–Yang–Parr (LYP) functional [27] with a small admixture of the Vosko–Wilk–Nusair (VWN) functional [28] was used as the correlation functional. The basis set was 6-31G* [29]. As was demonstrated by calculations for a great number of similar systems [30], the B3LYP/6-31G* approximation provides an adequate description of energetics (heat of reaction, reaction

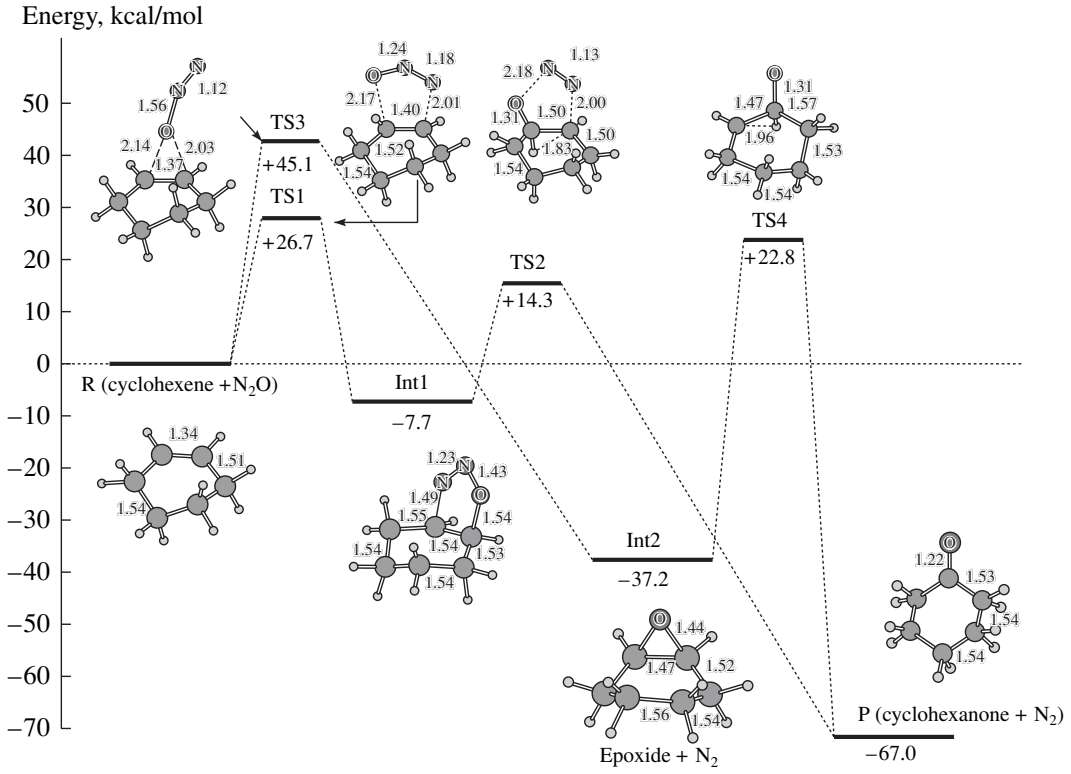

Fig. 1. Direct cyclohexene oxidation with nitrous oxide into an epoxide and cyclohexanone: energy diagram and intermediate structures at the stationary points of the reaction path. The zero point of energy is the energy of the reactants R.

path, activation energy, etc.) and structure (optimized geometry), including frequency analysis of normal modes. The zero-point energy was neglected in the reaction path analysis. Transition states were sought by the STQN method (QST2 and QST3 variants) [31]. The calculations were made using the Gaussian 98 program package [32].

THEORETICAL RESULTS

Cyclohexene + N_2O ⟶ Cyclohexanone + N_2

Figure 1 displays the energy diagram for this reaction, including the optimized structures of all transition complexes at stationary points. Tentative data calculated for this reaction were reported in an earlier publication [33]. In the upper part of the energy diagram, we show the structures of the transition states. The structures of the intermediates are shown in the lower part of the diagram. Below, we consider some electronic and structural properties of the initial reactants and the reaction products.

For N_2O, which is an asymmetric molecule, the N–N and N–O bond lengths are calculated to be 1.135 and 1.192 Å, respectively. These values are in strong agreement with experimental data (1.128 and 1.184 Å, respectively [34]). The N_2O molecule is a typical representative of the wide variety of 1,3-dipoles, which react with dipolarophiles to yield five-membered heterocycles [20]. At the same time, nitrous oxide shows both electrophilic and nucleophilic properties. This unique combination of properties is due to the fact that the following three resonance structures contribute to the energy of the ground state:

(a) $N{\equiv}N^+{-}O^-$; (b) $N^+{=}N{-}O^-$; (c) $N^-{=}N^+{=}O$.

According to our calculations, the effective Mulliken charges are $q_N = -0.119$, $q_{N(O)} = +0.618$, and $q_O = -0.499$. Since the negative charge of the terminal nitrogen atom is small, the main contribution to the energy of the ground state is made by structure (a), whose oxygen atom is a strong nucleophile. However, this structure is not involved in the reaction considered. The other structures define two possible reaction channels. The first involves the formation of the five-membered intermediate 1,2,3-oxadiazole (Int1). Here, the key role is played by structure (b), whose terminal atoms are oppositely charged, forming a 1,3-dipole. The second channel is through the formation of a three-membered epoxide, C–O–C (Int2). The key role in this channel is played by structure (c), whose oxygen atom has pronounced electrophilic properties.

In the cyclohexene molecule, the carbon atoms forming the C=C bond are sp^2-hybridized and the four

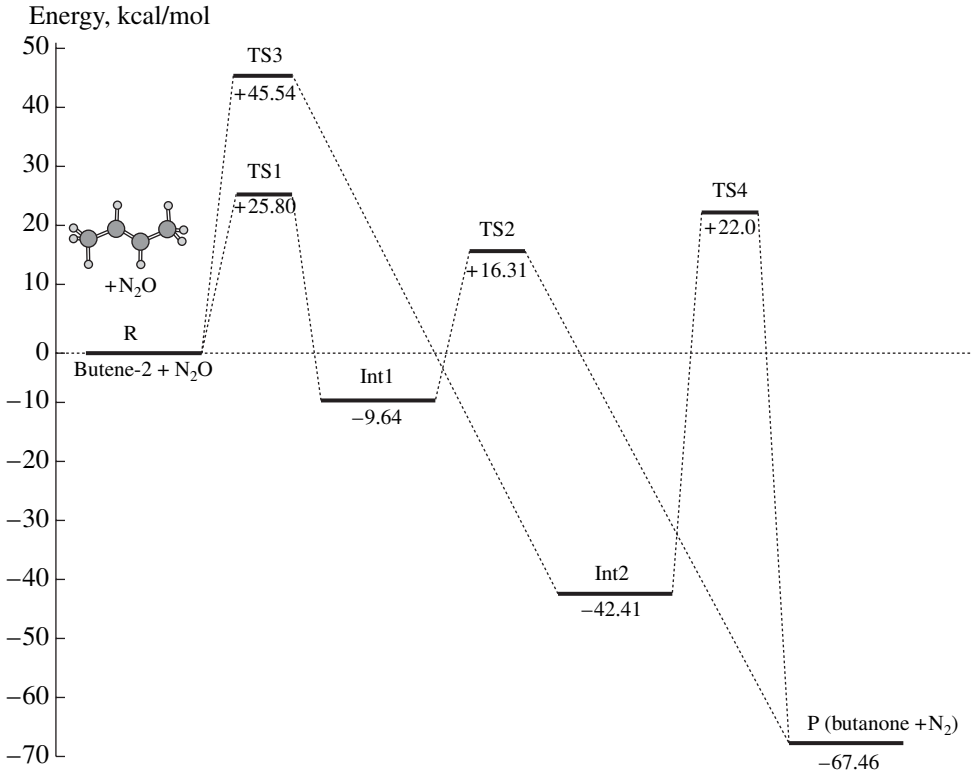

Fig. 2. Direct oxidation of butene-2 with nitrous oxide into butanone (P): energy diagram for the reaction channels passing through 1:2:3-oxadiazole (Int1) and an epoxide (Int2). The zero point of energy is the energy of butene-2 + N_2O.

other atoms are sp^3-hybridized, defining specific planar and tetrahedral arrangements of hydrogen atoms. Two conformations of the cyclohexene ring are possible, namely, a half-chair and a half-boat. According to our calculated data, the half-chair is more stable than the half-boat by ~2 kcal/mol. For cyclohexanone, the calculations predict two structural isomers, with *trans* and *cis* configurations of the carbon ring. The *trans* configuration is 4.1 kcal/mol more stable than the *cis* configuration. The activation energy for the *trans* ⟶ *cis* transition is E_{tc} = 17 kcal/mol. The most stable structures of cyclohexene and cyclohexanone are shown in Fig. 1.

Consider the structures of the intermediates. Direct interaction between the 1,3-dipole N^+=N–O^- and cyclohexene involves the C=C bond, giving a stable complex (Int1) including the five-membered heterocycle –C–N=N–O–C– of dihydro-1:2:3-oxadiazole (Fig. 1). The N–N and N–O distances (1.23 and 1.43 Å, respectively) are characteristic of the double bond N=N and the ordinary bond N–O. This type of complex has not been reported in the literature as yet, even though our calculations predict that the above complex is sufficiently more stable than the initial reactants (ΔH_1 = –7.7 kcal/mol) to be detectable at low temperatures.

The attack by the electrophilic oxygen of the N^-=N^+=O valent structure on the C=C bond of cyclohexene results in a rather stable compound (epoxide) with a formation energy of ΔE = –37.2 kcal/mol (Int2). In this case, a nitrogen molecule is released to the gas phase as early as in the first step. *Trans* and *cis* conformations of the carbon ring are possible. The oxygen atom is out of the ring plane. The C–O bond is shorter and the C–C bond is longer in the *trans* isomer than in the *cis* isomer. The latter is 2.5 kcal/mol more stable than the former.

The transformations of the reactants R into Int1 and Int2 are activated processes that can be represented as R ⟶ TS1 ⟶ Int1 and R ⟶ TS3 ⟶ Int2. Their activation energies are E^* = 27 and 45 kcal/mol, respectively, and are defined by the energies of the transition states TS1 and TS3. Calculation of vibration frequencies for TS1 and TS3 confirmed that the structures deduced correspond to first-kind saddles on the energy surface, the imaginary frequencies being ν(TS1) = 452i cm^{-1} and ν(TS3) = 844i cm^{-1}. As is clear from Fig. 1, the heterocycles TS1 and TS3 differ fundamentally in structure. In TS3, the N–N bond length (1.12 Å) is similar to that in the nitrogen molecule in the gas phase (1.11 Å) and the N–O distance (1.56 Å) means breaking of the N–O bond in the N_2O molecule. Unlike TS1, TS3 does not contain any nitrogen atoms. Due to these specific fea-

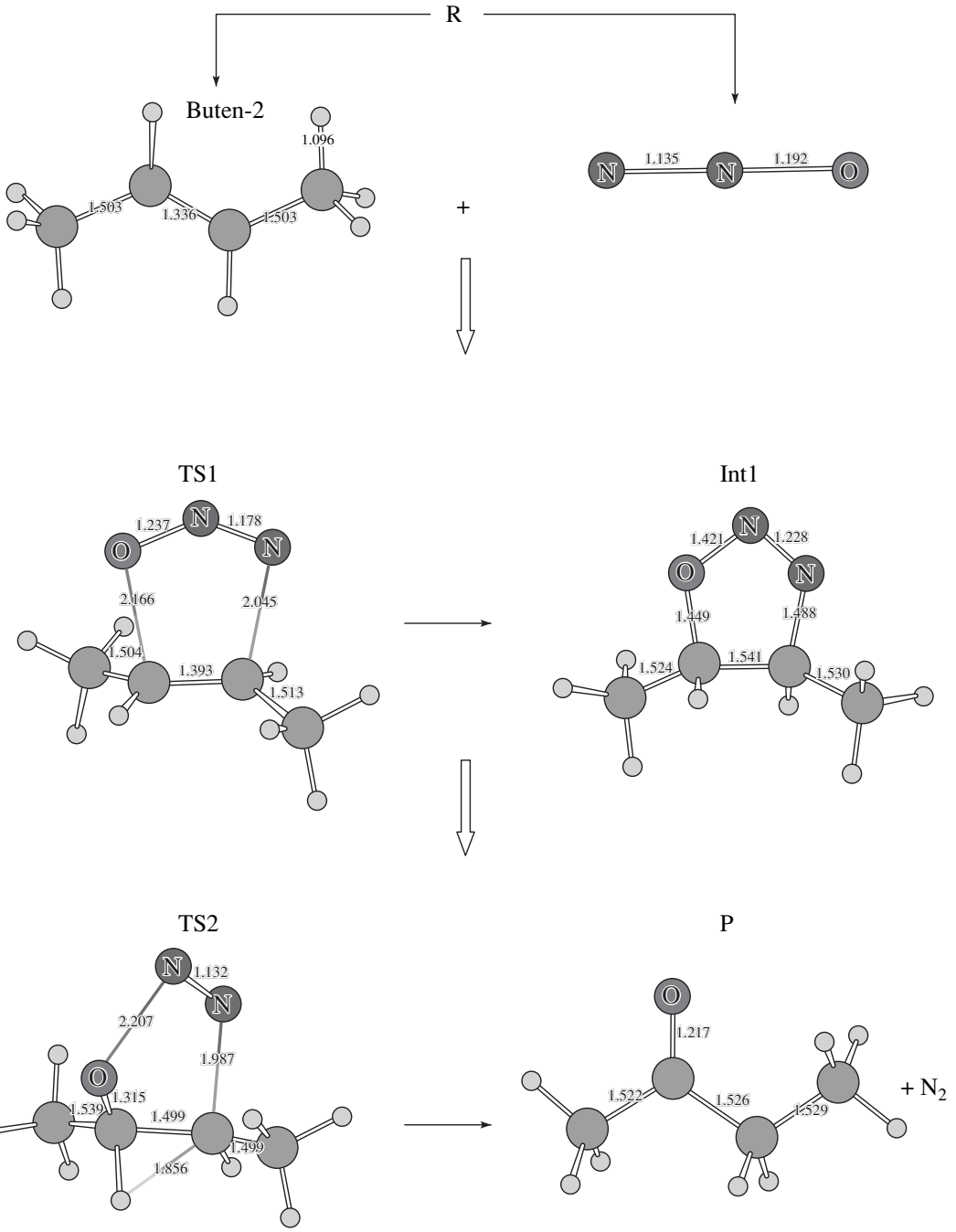

Fig. 3. Optimized structures of the reactants (R), intermediate (Int), transition states (TS's), and product (P) for the reaction channel R ⟶ TS1 ⟶ Int1 ⟶ TS2 ⟶ P.

tures of the TS3 structure, the second channel, which includes epoxide formation, is characterized by a high activation energy. It is believed that the second channel is possible only at very high temperatures, as opposed to the catalytic liquid-phase alkene oxidation with nitrous oxide into epoxides [35, 36].

The reaction path of the first channel (through Int1) is energetically more favorable. We studied the formation of TS1 by scanning the C–ON_2 bond distance (r). For $r > 3.0$ Å, the CON angle is approximately 180° and the parameters of the N_2O molecule are similar to the parameters of this molecule in the gas phase. For $r < 3.0$ Å, the CON angle decreases to 90° as the reactants are brought closer together, and the NNO angle displays a similar decrease. At $r = 2.17$ Å, the system is in the transition state TS1, which has the following

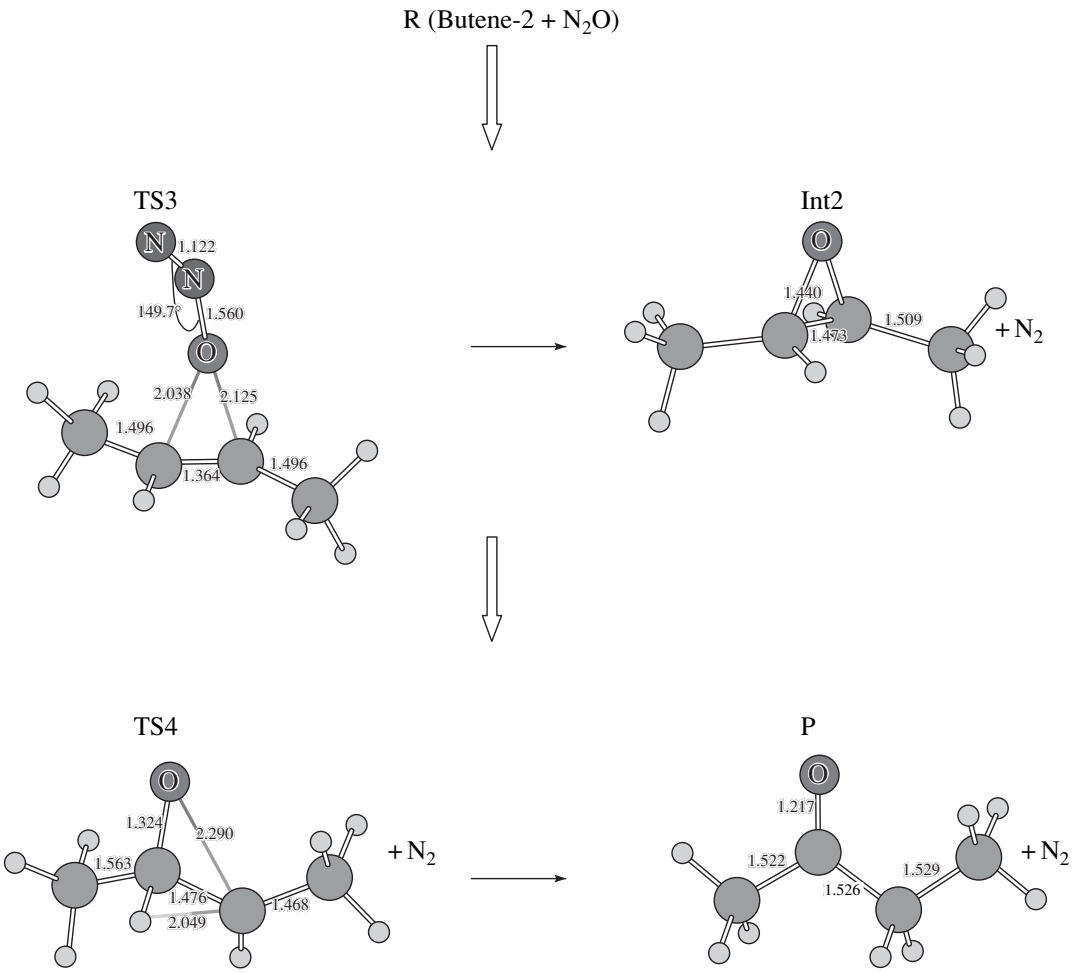

Fig. 4. Optimized structures of the reactants (R), intermediate (Int2), transition states (TS's), and product (P) for the reaction channel R ⟶ TS3 ⟶ Int2 ⟶ TS4 ⟶ P.

parameters: N–N, 1.18 Å; N–O, 1.24 Å; C–N, 2.01 Å; C–C, 1.40 Å; and ∠NNO, 135°. Note that very similar parameters were calculated for N_2O cycloaddition to ethylene [21] and, as is demonstrated below, for the same reaction with butene-2. It is, therefore, believed that the oxidations of cyclic and aliphatic alkenes pass through structurally similar transition states in their first steps.

The possible second-step conversions are Int1 ⟶ TS2 ⟶ P and Int2 ⟶ TS4 ⟶ P. We consider only cyclohexanone (+N_2) as the product. The structures of TS2 and TS4 are presented in Fig. 1. Frequency analysis of the normal modes demonstrated that these structures are true transition states with imaginary frequencies of ν(TS2) = 437i cm^{-1} and ν(TS4) = 690i cm^{-1}. The Int2 ⟶ TS4 ⟶ P path, which requires an activation energy of $E^* > 60$ kcal/mol, is implausible and can be ruled out for the liquid phase. By contrast, the Int1 ⟶ TS2 ⟶ P channel, which requires a lower activation energy of $E^* \sim 22$ kcal/mol, will be open for cyclohexanone formation, and the heat ΔH of the overall reaction R ⟶ TS1 ⟶ Int1 ⟶ TS2 ⟶ P will be −67 kcal/mol. Therefore, for the first channel leading to the ketone, the reaction rate is controlled by the first step, whose activation energy is $E^* \sim 22$ kcal/mol (Fig. 1).

Butene-2 + N_2O ⟶ Methyl Ethyl Ketone + N_2

Figure 2 presents an energy diagram for the direct oxidation of butene-2 with nitrous oxide into methyl ethyl ketone, including reaction channels via a 1:2:3-oxadiazole (Int1) and an epoxide (Int2). Comparing Figs. 1 and 2 clearly demonstrates that identical energy profiles are calculated for the butene-2 and cyclohexene oxidations into the corresponding ketones. As compared to cycloalkenes, linear alkenes symmetric with respect to the C=C bond have some specific features. All intermediates in butene-2 conversion are more stable than the intermediates in cyclohexene conversion.

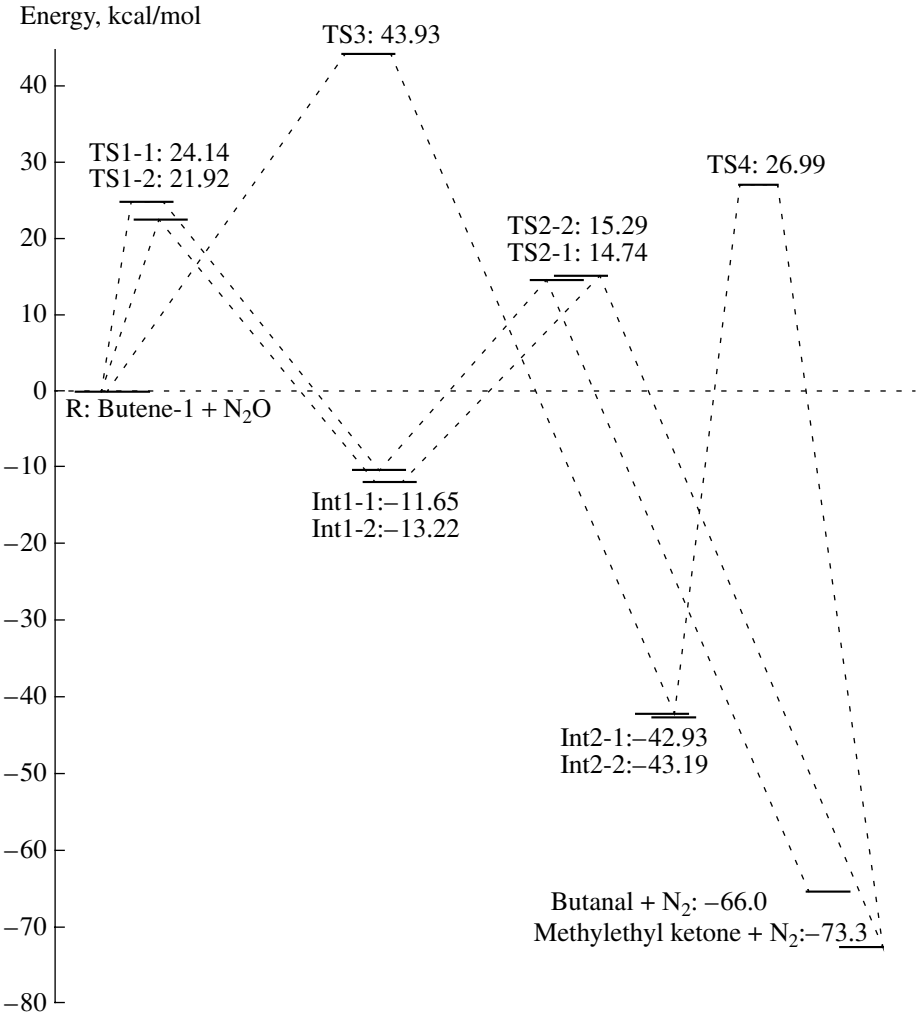

Fig. 5. Direct oxidation of butene-1 with nitrous oxide: energy diagram for the reaction channels involving Int1-1, Int1-2, and Int2. The zero point of energy is the energy of butene-1 + N_2O.

Furthermore, the second-step activation energy is higher in the former reaction than in the latter for both reaction channels considered. Therefore, the probability of a reaction channel leading to a product other than ketone is higher for butene-2 than for cyclohexene. As a consequence, ketone selectivity will be higher for butene-2 oxidation than for cyclohexene oxidation.

Figure 3 shows the optimized structures of the reactants (butene-2 and nitrous oxide), intermediates, transition states, and methyl ethyl ketone (butanone-2) for the first reaction path, R ⟶ TS1 ⟶ Int1 ⟶ TS2 ⟶ P. Figure 4 displays the optimized structures for the second reaction path, R ⟶ TS3 ⟶ Int2 ⟶ TS4 ⟶ P. Comparison of the transition-state structures at stationary points of the reaction paths suggests that the mechanisms of oxygen transfer from N_2O to the C=C bond of cyclohexene and butene-2 are essentially the same—an inference of practical significance. The reaction of butene-2 is controlled by the first step of the first path, whose activation energy is E^* ~ 25.8 kcal/mol (Fig. 2). This value corresponds well with experimental data (E^*_{exp} = 22 kcal/mol [37]). The second channel in butene-2 oxidation, which is via an epoxide, is as unlikely as the second path in cyclohexene oxidation.

Butene-1 + N_2O ⟶ Methyl Ethyl Ketone (Butanal) + N_2

Unlike butene-2, butene-1, in which the C=C bond is terminal, allows two energetically similar reaction pathways within the first reaction channel, one leading to a ketone and the other to an aldehyde. Figure 5 shows the energy diagrams for direct butene-1 oxidation with nitrous oxide via 1:2:3-oxadiazole (Int1) and an epoxide (Int2). For the first channel, there can be two reaction pathways differing in the orientation of the N=N–O molecule relative to the C=C bond of butene-1.

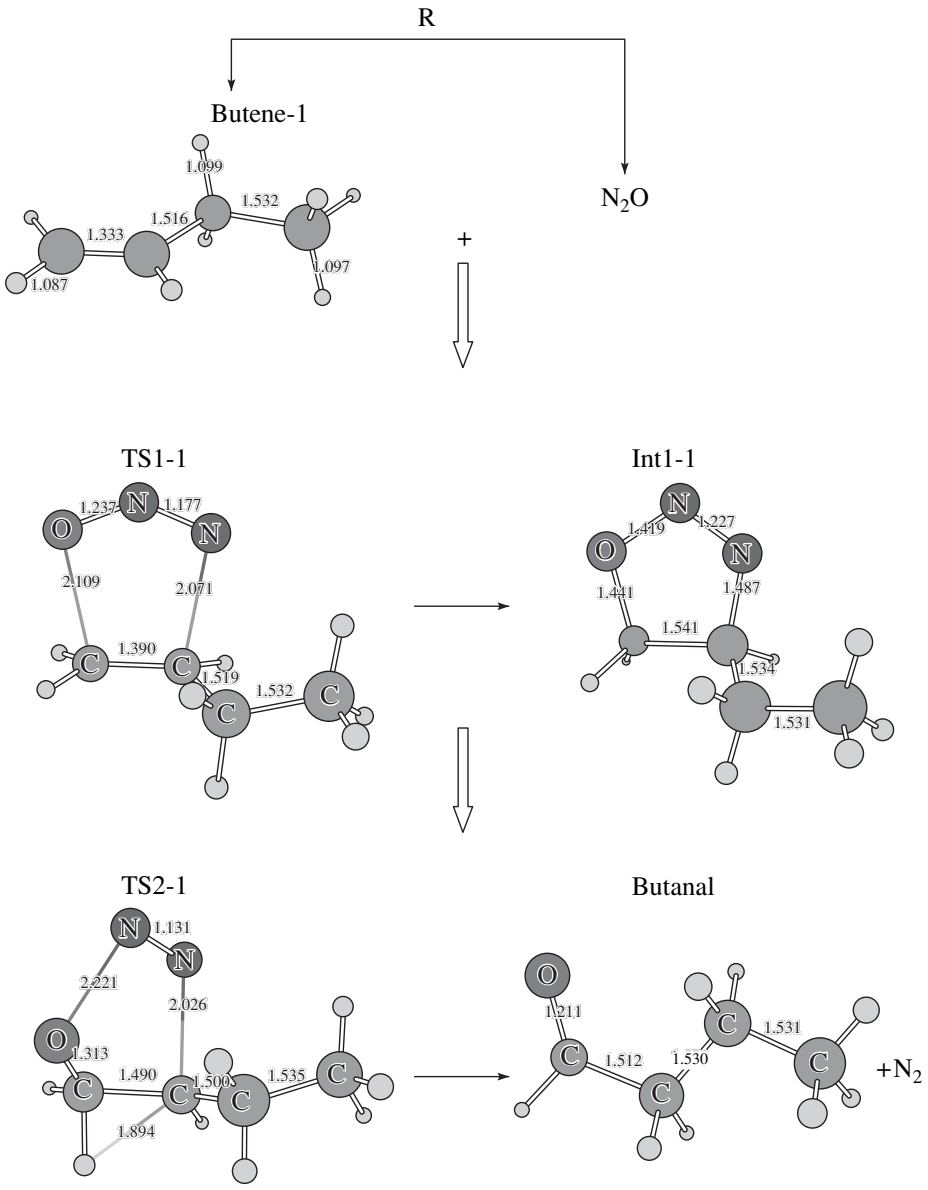

Fig. 6. Optimized structures of the intermediates and transition states resulting from attack by the oxygen of N_2O on the first carbon atom of butene-1 (reaction channel butene-1 + N_2O ⟶ TS1-1 ⟶ Int1-1 ⟶ TS2-1 ⟶ butanal + N_2).

The first pathway, which includes the TS1-1 ⟶ Int1-1 ⟶ TS2-1 transformations, leads to butanal. The second pathway, which includes TS1-2 ⟶ Int1-2 ⟶ TS2-2, ends in methyl ethyl ketone. Figure 6 displays the structures of the intermediates resulting from the attack of the oxygen atom of N_2O on the first carbon atom of butene-1. This reaction pathway leads to butanal. Figure 7 presents the intermediate structures resulting from the same attack on the second carbon atom of butene-1. In this case, the C=O bond forms at the second carbon atom of butene-1 and the final oxidation product is methyl ethyl ketone. In Fig. 8, we show the intermediate structures that result from the attack of the electrophilic oxygen of N_2O on the middle of the C=C bond. This is the second channel of butene-1 oxidation, which passes through the transition states TS3 and TS4 and the intermediate Int2 (epoxide). As in the case of butene-2, this channel is energetically implausible. Furthermore, butene-2 and butene-1 form structurally identical transition states and intermediates (see Figs. 4 and 8).

Thus, our calculations predict two possible pathways for the first channel of direct butene-1 oxidation with nitrous oxide. These pathways involve energetically similar intermediates and transition states, but they lead to different final products, namely, a ketone and an aldehyde. Both pathways consist of two steps.

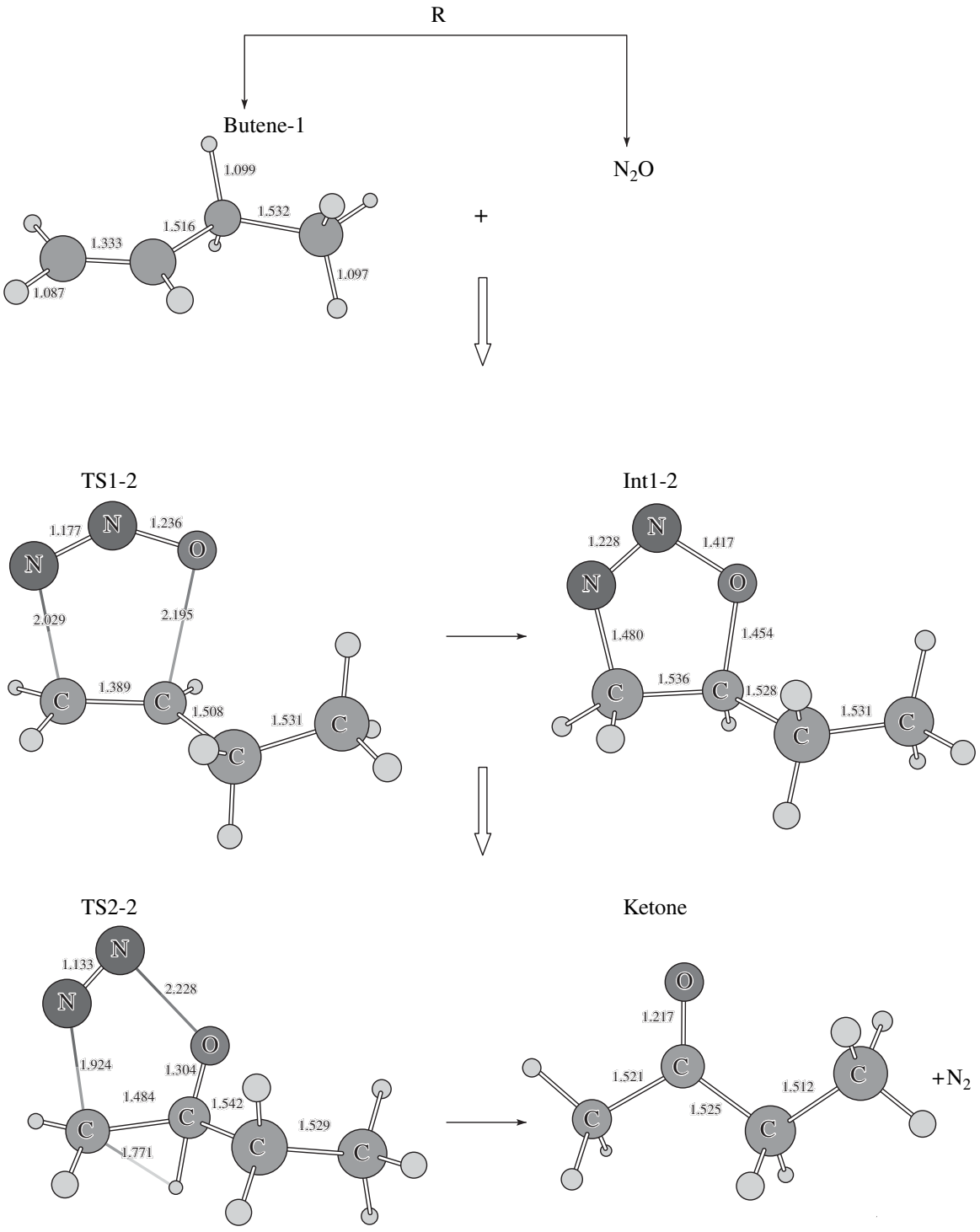

Fig. 7. Optimized structures of the intermediates and transition states resulting from attack by the oxygen of N_2O on the second carbon atom of butene-1 (reaction channel butene-1 + N_2O ⟶ TS1-2 ⟶ Int1-2 ⟶ TS2-2 ⟶ methyl ethyl ketone + N_2).

According to our calculations, the first-step activation energies are E^* = 22 and 24 kcal/mol and the second-step energies are E^* = 28 and 27 kcal/mol for the ketone and aldehyde, respectively. The corresponding energies of the overall reaction are –73.3 and –66.0 kcal/mol (see Fig. 5). Note that the effective activation energy is counted from the energy of the initial reactants. Therefore, the second-step activation energy is ~15 kcal/mol for both pathways (see Fig. 5). Hence, the first step, with E^* = 22–24 kcal/mol, is rate-limiting in this reac-

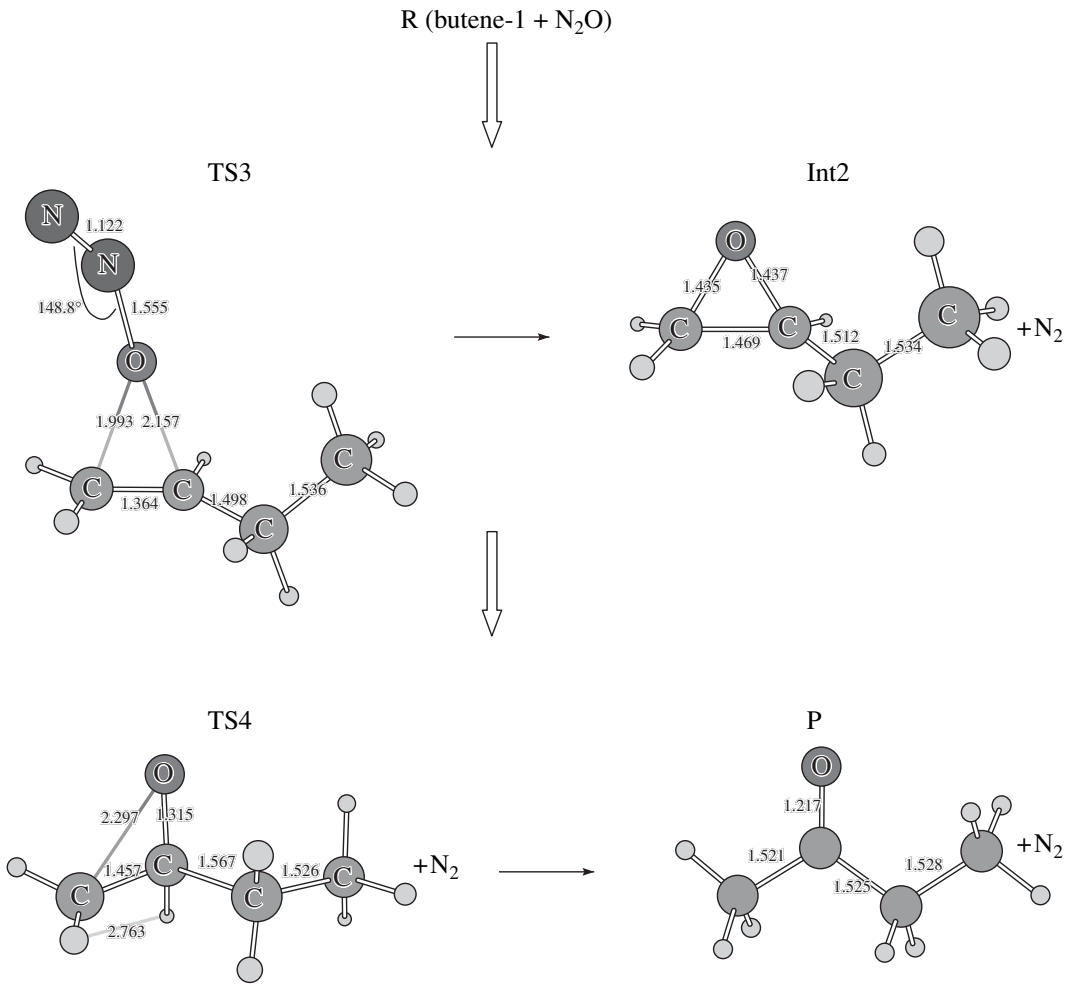

Fig. 8. Optimized structures of butene-1, epoxide (Int2), transitions states (TS's), and ketone (P) for the reaction channel R ⟶ TS3 ⟶ Int1 ⟶ TS4 ⟶ P.

tion. The experimental activation energy E^*_{exp} for butene-1 and butene-2 is 22 kcal/mol. In the case of butene-1, as opposed to butene-2, the existence of two energetically similar pathways will markedly reduce the ketone selectivity of the reaction. Since the activation energy for the aldehyde pathway is estimated to be only 2 kcal/mol above the activation energy for the ketone pathway, the reaction product will be dominated by the ketone, but it will contain a considerable proportion of the aldehyde. Domination of methyl ethyl ketone over butanal is observed experimentally: between 180 and 240°C, the ketone-to-aldehyde ratio is 3 : 1 [37].

DISCUSSION

Cyclohexene oxidation into cyclohexanone was the first success in selective liquid-phase alkene oxidation with nitrous oxide [14]. Later, similar reactions were carried out for a variety of compounds, including aliphatic alkenes [15, 16]. Two hypothetical mechanisms of oxygen transfer from N_2O to the C=C bond of the alkene were considered. The first hypothesis is based on the assumption that oxidation first provides an epoxide, which then undergoes isomerization into a ketone:

$$R{-}CH{=}CH{-}R + N_2O \longrightarrow R{-}\overset{\displaystyle O}{\overset{/\ \backslash}{CH{-}CH}}{-}R + N_2 \longrightarrow R{-}CH_2{-}\overset{\displaystyle O}{\overset{\|}{C}}{-}R + N_2. \qquad \text{(III)}$$

According to the second hypothesis [17, 18], an oxygen atom is transferred through the 1,3-dipolar cycloaddition of N_2O to the C=C bond. Next, the resulting intermediate decomposes, yielding a ketone and releasing N_2 to the gas phase:

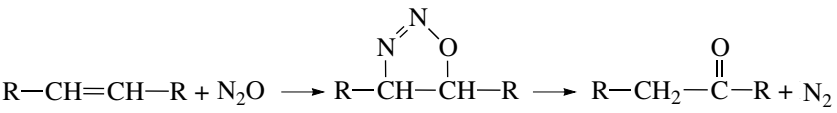

(IV)

Experimental investigation of cyclohexene oxidation demonstrated that the epoxide does not form under the reaction conditions and, if introduced into the reaction mixture, will remain unreacted [14]. Our calculations provide a plausible explanation for this finding. As is noted above, the activation energy for epoxide formation via TS3 is $E^* > 40$ kcal/mol. This value exceeds the N–O bond dissociation energy in the free N_2O molecule; therefore, this mechanism is impossible in the liquid phase. Even if the epoxide is introduced into the reaction mixture (i.e., the first step is skipped), its subsequent isomerization into the ketone (the second step) will require an activation energy of $E^* > 60$ kcal/mol (Figs. 1, 5). Thus, our calculations predict that this reaction will consist of two steps and proceed through the formation of the five-membered heterocycle of 1,2,3-oxadiazole.

The first step can be viewed as activation of oxygen in the N_2O molecule; accordingly, the structural changes in the activated complex are mainly limited to the heterocycle. The second step includes hydrogen transfer within the hydrocarbon moiety: $HC_1–C_2H \longrightarrow H_2C_1–C_2$. As a consequence, the greatest deformation takes place in the hydrocarbon backbone. Since the first step is rate-limiting, cycloalkenes and aliphatic alkenes symmetric with respect to the C=C bond will be oxidized by similar mechanisms, yielding a ketone as the main product. However, a quite different situation is observed for alkenes with a terminal C=C bond. As is noted above, two energetically similar oxidation pathways are predicted for butene-1, implying a decrease in the ketone selectivity of the reaction. The activation energy data calculated for the separate reaction steps suggest that the ketone pathway is energetically favorable and the ketone selectivity decreases in the order butene-2 > butene-1. The ratio between the butene-1 activation energies for the first and second pathways suggests that the ketone selectivity may decrease slightly with increasing temperature because of the increasing proportion of the aldehyde in the final product.

CONCLUSION

The reaction path analysis for N_2O–alkene interaction demonstrates the possibility of direct noncatalytic alkene oxidation into carbonyl compounds under mild conditions. This result is in good agreement with recent experimental data. This reaction is due to the ability of nitrous oxide to interact with the double bond of the alkene by a 1,3-dipolar cycloaddition mechanism, yielding a 1,2,3-oxadiazoline intermediate complex that is decomposable to a carbonyl compound.

ACKNOWLEDGMENTS

The authors thank G.I. Panov and K.A. Dubkov for their interest in this study and for discussion of the results.

This study was supported by the Presidium of the Russian Academy of Sciences through the Directed Synthesis of Compounds with Desired Properties and Preparation of Functional Materials Program (project 9.3).

This study was also sponsored through the Support to Leading Scientific Schools Program (grant no. 1140.2003.3).

REFERENCES

1. Panov, G.I., *CATTECH*, 2000, vol. 4, p. 18.
2. Leontiev, A.V., Fomicheva, O.A., Proskurnina, M.V., and Zefirov, N.S., *Russ. Chem. Rev.*, 2001, vol. 70, p. 91.
3. Ross, S.K., Sutherland, J.W., Kuo, S.-C., and Klemm, R.B., *J. Phys. Chem.*, 1997, vol. 101, p. 1104.
4. Panov, G.I., Uriarte, A.K., Rodkin, M.A., and Sobolev, V.I., *Catal. Today*, 1998, vol. 41, p. 365.
5. Delabie, A., Vinckier, C., Flock, M., and Pierloot, K., *J. Phys. Chem. A*, 2001, vol. 105, p. 5479.
6. Yoshizawa, K., Yumura, T., Shiota, Y., and Yamabe, T., *Bull. Chem. Soc. Jpn.*, 2000, vol. 73, p. 29.
7. Kachurovskaya, N.A., Zhidomirov, G.M., Hensen, E.J.M., and van Santen, R.A., *Catal. Lett.*, 2003, vol. 86, p. 25.
8. Ryder, J.A., Chakraborty, A.K., and Bell, A.T., *J. Phys. Chem. B*, 2002, vol. 106, p. 7059.
9. Yakovlev, A.L., Zhidomirov, G.M., and van Santen, R.A., *Catal. Lett.*, 2001, vol. 175, p. 45.
10. Yakovlev, A.L. and Zhidomirov, G.M., *Catal. Lett.*, 1999, vol. 63, p. 91.
11. Filatov, M.Y., Pelmenschikov, A.G., and Zhidomirov, G.M., *J. Mol. Catal.*, 1993, vol. 80, p. 243.
12. Arbuznikov, A.V. and Zhidomirov, G.M., *Catal. Lett.*, 1993, vol. 40, p. 17.
13. Yakovlev, A.L., Zhidomirov, G.M., and van Santen, R.A., *J. Phys. Chem. B*, 2001, vol. 105, p. 12297.
14. Panov, G.I., Dubkov, K.A., Starokon, E.V., and Parmon, V.N., *React. Kinet. Catal. Lett.*, 2002, vol. 76, p. 401.
15. Dubkov, K.A., Panov, G.I., and Starokon, E.V., *React. Kinet. Catal. Lett.*, 2002, vol. 77, p. 197.
16. Starokon, E.V., Dubkov, K.A., Babushkin, D.E., Parmon, V.N., and Panov, G.I., *Adv. Synth. Catal.*, 2004, vol. 346 (in press).
17. Bridson-Jones, F.S., Buckley, G.D., Cross, L.H., and Driver, A.P., *J. Chem. Soc.*, 1951, p. 2999.
18. Bridson-Jones, F.S. and Buckley, G.D., *J. Chem. Soc.*, 1951, p. 3009.
19. Buckley, G.D. and Levy, W.J., *J. Chem. Soc.*, 1951, p. 3016.

20. Huisgen, R., *1,3-Dipolar Cycloaddition Chemistry*, Padwa, A., Ed., New York: Wiley, 1984, vol. 1.
21. Su, M.D., Liao, H.Yi., Chung, W.S., and Chu, S.Y., *J. Org. Chem.*, 1999, vol. 64, p. 6710.
22. Gonzalez, C. and Schlegel, H.B., *J. Phys.Chem.*, 1990, vol. 94, p. 5523.
23. Parr, R.G. and Yang, W., *Density-Functional Theory of Atoms and Molecules*, New York: Oxford Univ. Press, 1989.
24. Kohn, W., Becke, A.D., and Parr, R.G., *J. Phys. Chem.*, 1996, vol. 100, p. 12974.
25. Becke, A.D., *Phys. Rev. A*, 1988, vol. 38, p. 3098.
26. Becke, A.D., *J. Chem. Phys.*, 1993, vol. 98, p. 5648.
27. Lee, C., Yang, W., and Parr, R.G., *Phys. Rev. B: Condens. Matter*, 1988, vol. 37, p. 785.
28. Vosko, S.H., Wilk, L., and Nusair, M., *Can. J. Phys.*, 1980, vol. 58, p. 1200.
29. Krishnan, R., Seger, J.S., and Pople, J.A., *J. Chem. Phys.*, 1980, vol. 72, p. 650.
30. Baker, J., Muir, M., Andzelm, J., and Scheiner, A., *Chemical Applications of Density Functional Theory*, Laird, B.B., Ross, R.B., and Ziegler, T., Eds., ACS Symp. Ser., 1996, no. 629.
31. Peng, C., Ayala, P.Y., Schlegel, H.B., and Frisch, M.J., *J. Comput. Chem.*, 1996, vol. 17, p. 49.
32. Frisch, M.J., Trucks, G.W., Schlegel, H.B., *et al.*, *Gaussian: Revision A.11*, Pittsburgh, 2001.
33. Avdeev, V.I., Ruzankin, S.Ph., and Zhidomirov, G.M., *Chem. Commun.*, 2003, p. 42.
34. Amioot, C., *J. Mol. Spectrosc.*, 1976, vol. 59, p. 380.
35. Yamada, T., Hashimoto, K., Kitaichi, Y., Suzuki, K., and Ikeno, T., *Chem. Lett.*, 2001, vol. 3, p. 268.
36. Ben-Daniel, R., Weiner, L., and Neumann, R., *J. Am. Chem. Soc.*, 2002, vol. 124, p. 8788.
37. Semikolenov, S.V., Dubkov, K.A., Starokon', E.V., Babushkin, D.E., and Panov, G.I., *Izv. Akad. Nauk, Ser. Khim.*, 2005 (in press).